Research on a Robust Adaptive Controller with Disturbance Observer For Wheeled Mobile Robot

Submitted: 16th September 2024; accepted: 4th November 2025

Trong Tai Nguyen, Doan Phuc An Nguyen, Dai Nghia Tran, Phuc Bao Nguyen Nguyen, Thanh Dat Mai

DOI: 10.14313/jamris-2026-001

Abstract:
This paper presents a robust adaptive controller for wheeled mobile robots (WMRs) designed to effectively compensate for disturbances and system uncertainties. The proposed control scheme includes an inner loop with a PID controller for wheels speed control and an outer loop with a disturbance observer to track the trajectory and minimize position errors. The outer loop control signal is derived based on the WMR's dynamic and kinematic models, while the disturbance observer adapts to uncertainties and external disturbances. The system's stability is proven in sense of Lyapunov theory. The performance of the proposed controller is validated through simulations, which show significant improvements in trajectory tracking compared to existing methods. Furthermore, experimental results confirm that the controller maintains stability and robustness under varying load conditions and different trajectory paths, demonstrating its effectiveness in real-world applications.

Keywords: *Wheeled Mobile Robot (WMR), Lyapunov Stability, Disturbance Observer, Adaptive Control, WMR Dynamic*

1. Introduction

Wheeled Mobile Robot (WMR) refers to robots that navigate on the ground using motorized wheels to propel themselves. Among the branches of mobile robots, WMRs are simpler and more efficient than other designs, such as those that utilize grooves or legged robots. They are easy to design, produce, and program for linear and angular motion on a horizontal plane. This makes the WMRs an active field of research in order to fulfill the needs of surveys, patrols, emergency savings, identification, petrochemicals in automation, building structures, transportation, and healthcare. With numerous features, WMRs are being applied in various fields such as agriculture services and other industries [1–7]. Since then, the requirements for accurately controlling the movement trajectory of mobile robots with wheels have also increased.

Experiments show that between the two main types of WMR, nonholonomic robots are more difficult to control than holonomic robots [8]. Hence, this kind of system poses more problems for researchers.

The trajectory accuracy of holonomic robots is affected by various uncertain factors from the robot itself and external forces, making it more challenging to control the system [9].

To address these challenges, various solutions have been proposed to enhance the accuracy and trajectory tracking of nonholonomic wheeled mobile robots (WMRs) under uncertain interference factors. These solutions include fuzzy control [10–12], backsteppingbased control [13–15], and sliding mode control (SMC) [16–18], among others [5, 12, 19–21]. However, controllers based on the "no-slip wheel" hypothesis, such as SMC [16, 18, 22], adaptive control [23–26], and backstepping control [13,14], fail to meet the system's requirements for stability and precise trajectory tracking.

In recent years, several methods have been proposed to solve interference problems in WMR control. One of them is robust adaptive tracking control [26–28], a tracking controller that combines disturbance observer and a responsive compensation mechanism to deal with unstable systems. Therefore, the errors and responses are limited. In [29], the problem of trajectory tracking for WMR under conditions of system uncertainty and external disturbances was solved. By using a fuzzy logic system (FLS) for model estimation and an adaptive fuzzy observer for estimating unmeasured velocities, the position errors are minimized and system response is fast.

Wheel slips in WMR are also an interesting problem for many researchers. In order to overcome the challenges in a conventional backstepping controller, a dynamic surface controller (DSC) is developed [5, 30], which incorporates skidding and sliding mechanisms. In [17], a control scheme combining sliding mode control with a backstepping observer is proposed for WMRs with unknown sliding and model uncertainty. This algorithm mitigates the effects of system uncertainties, disturbances, and vibrations inherent in sliding mode control; however, the illustrative results are not satisfactory. A control technique utilizing a fuzzy PID controller, combined with IMU and feedback current, is introduced in [31] to reduce slippage caused by environmental factors. While the results indicate that this control scheme is effective, system stability is not addressed. In [17, 32], a controller based on a disturbance observer that accounts for skidding and sliding is presented, however the error in this algorithm remains significantly high.

The robust adaptive controller developed in [33] accounts for disturbances and wheel slips, with the WMR dynamics explicitly considering wheel slip in the tracking controller's design. A disturbance observer is utilized to estimate robot uncertainties and slip. However, the controller has only been verified through simulations, and the discontinuous transition in the control law may lead to instability.

This paper aims to deal with the shortcomings of the approach presented in [33] for tracking control of Wheeled Mobile Robots (WMRs). The proposed control scheme consists of two loops: an inner loop, which uses a PID controller for precise wheel speed regulation, and an outer loop, which employs a disturbance observer to accurately track the reference trajectory in case of disturbances and uncertainties. The key contributions of this paper are as follows:

- **Improvement of [33]:** The outer loop tracking controller is re-derived using Lyapunov stability theory, and a novel method for handling noninvertible matrices is introduced.
- **Simulation Validation:** The proposed control structure is thoroughly tested in simulations, demonstrating significant improvements in system response compared to the method in [33].
- **Experimental Verification:** The effectiveness of the proposed scheme is further validated through realworld experiments on a WMR, with the results confirming its superior performance.

2. Wheeled Mobile Robot Model

In this research, the WMR model is referred from [33], the kinematics and dynamics model of WMR, which takes account of wheel slips, and is summarized as follows:

$$\begin{cases} \dot{x}_M = \vartheta \cos(\theta) - \dot{\eta} \sin(\theta) \\ \dot{y}_M = \vartheta \sin(\theta) + \dot{\eta} \cos(\theta) \\ \dot{\theta} = \omega \end{cases} \tag{1}$$

$$I\dot{v} + Bv + Q\ddot{\gamma} + C\dot{\eta} + G\ddot{\eta} + \tau_d = \tau \tag{2}$$

where ϑ, ω are the WMR forward velocity and angular velocity at midpoint of driving wheels M, respectively, which is determined as:

$$\vartheta = \frac{r\left(\dot{\phi}_R + \dot{\phi}_L\right)}{2} + \frac{\dot{\gamma}_R + \dot{\gamma}_L}{2}, \omega = \frac{r\left(\dot{\phi}_R - \dot{\phi}_L\right)}{2b} + \frac{\dot{\gamma}_R - \dot{\gamma}_L}{2b} \tag{3}$$

The robot parameters are defined and shown in Fig. 1. In which, $G\ (x_G, y_G)$ is the center of mass of the WMR platform, $M\ (x_M, y_M)$ is the midpoint of the driving wheels, $D\ (x_D, y_D)$ is the desired position; θ is the orientation of WMR; $2b$ is the width of WMR; r is the wheel radius; e_{p1}, e_{p2} are the position errors between M and D in the MXY coordinate; a is the distance between M and G; γ_R, γ_L are longitudinal slip factors of the right and left driving wheels, respectively; η is the lateral slip factor along the wheel shaft; I, B, Q, C and G are weighting matrices and vectors in WMR dynamic, which are defined in details in [33]:

3. Development of Controller

Similar to the approach in [33], the control scheme for the WMR consists of two loops arranged as a cascade control system, as shown in Fig. 2. The outer loop is responsible for controlling the robot's position. This controller incorporates a disturbance observer to compensate for disturbances, system uncertainties, and model errors. Meanwhile, the inner loop manages wheel speed control, ensuring that the wheels follow the speed commands generated by the outer loop.

The PID controller, known for its wide application due to its stability, robustness, and reliable control performance, is used in the inner loop. As a result, the overall control system heavily depends on the effectiveness of the outer loop controller. Therefore, this section focuses on the outer loop controller and the integration of the disturbance observer to enhance system performance.

3.1. Robot position tracking control

In the MXY coordinate, the errors between the robot position $M\ (x_M, y_M)$ and its desired point $D\ (x_D, y_D)$ are determined as:

$$e_p = \begin{bmatrix} e_{p1} \\ e_{p2} \end{bmatrix} = T \begin{bmatrix} x_D - x_M \\ y_D - y_M \end{bmatrix} \tag{4}$$

where $T = \begin{bmatrix} \cos(\theta) & \sin(\theta) \\ -\sin(\theta) & \cos(\theta) \end{bmatrix}$

Taking derivative of (4) with respect to time, it can be obtained as [33]:

$$\dot{e}_p = \begin{bmatrix} \dot{e}_{p1} \\ \dot{e}_{p2} \end{bmatrix} = T \begin{bmatrix} \dot{x}_D \\ \dot{y}_D \end{bmatrix} + h(.)v + d(.) \tag{5}$$

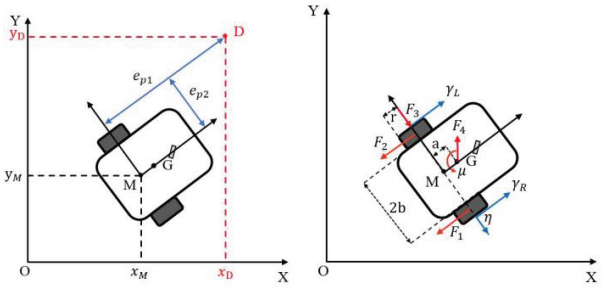

Figure 1. WMR in coordinates and its dynamic factors

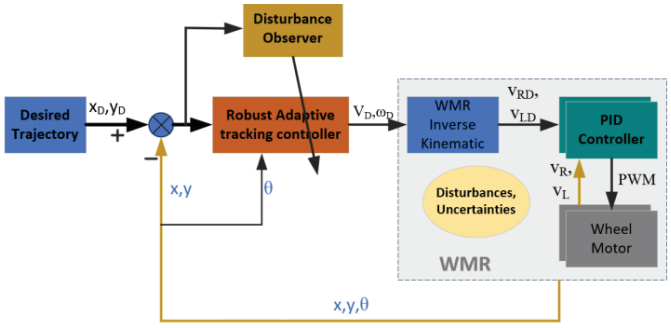

Figure 2. Overall structure of proposed control scheme

or

$$\dot{e}_p = T\dot{r}_D + h(.)v + d(.) \tag{6}$$

where $v = \left[\dot{\phi}_R \dot{\phi}_L\right]^T$ is the vector rotational speeds of right and left driving wheels; $\dot{r}_D = [\dot{x}_D \dot{y}_D]^T$; $h(.)$ *and* $d(.)$ *are two* matrices, that are determined as follows:

$$h(.) = \begin{bmatrix} \left(\frac{e_{p2}}{b} - 1\right)\frac{r}{2} & -\left(\frac{e_{p2}}{b} + 1\right)\frac{r}{2} \\ -\frac{e_{p1}r}{2} & \frac{e_{p1}r}{2} \end{bmatrix} \tag{7}$$

$$d(.) = \begin{bmatrix} \left(\frac{\dot{\gamma}_R - \dot{\gamma}_L}{2b}\right)e_{p2} - \left(\frac{\dot{\gamma}_R + \dot{\gamma}_L}{2}\right) \\ -\left(\frac{\dot{\gamma}_R - \dot{\gamma}_L}{2b}\right)e_{p1} - \dot{\eta} \end{bmatrix} \tag{8}$$

Then, the objective of the WMR control is to find the control rule for v so that e_p converges to zero.

3.2. Tracking control signal

When the WMR follows the reference, the position errors along x and y directions converge to zero. Hence, to find the control rule for position controller, the Lyapunov candidate function is chosen as:

$$V = e_p^T e_p \tag{9}$$

$$\dot{V} = e_p^T \dot{e}_p \tag{10}$$

From (6), it can be obtained:

$$\dot{V} = e_p^T \left[T\dot{r}_D + h(.)v + d(.)\right] \tag{11}$$

From (11), the control law v is selected as:

$$v = -h^{-1}(.)\left[\lambda e_p + T\dot{r}_D + d(.)\right] \tag{12}$$

where $\lambda = \begin{bmatrix} \lambda_1 & 0 \\ 0 & \lambda_2 \end{bmatrix}, \lambda_1, \lambda_2 > 0.$

Then (11) becomes:

$$\dot{V} = -e_p^T \lambda e_p < 0 \tag{13}$$

Thus, the system is asymptotic stable with the control law in (12) and e_p converges to zero in term of Lyapunov stable criteria.

From (11), the term $d(.)$ is an unknown factor, thus the control signal cannot be calculated directly. In this research the disturbance observer in [34] is employed to estimate this term.

3.3. Disturbance observer

Consider the system (6), the disturbance observer [34] is designed as:

$$\begin{cases} \dot{z} = -L\left(z + Le_p\right) - L\left[T\dot{r}_D + h(.)v\right] \\ \hat{d} = z + Le_p \end{cases} \tag{14}$$

The disturbance estimation error is defined as:

$$e_d = d - \hat{d} \tag{15}$$

Then the derivative of this error can be determined as:

$$\dot{e}_d = \dot{d} - \dot{\hat{d}} = \dot{z} + L\dot{e}_p \tag{16}$$

From (14) and (16), it is easy to obtain:

$$\dot{e}_d = \dot{d} - Le_d \tag{17}$$

It is assumed that the disturbance is low variation, then $\dot{d} \approx 0$ and $\dot{e}_d$ becomes:

$$\dot{e}_d \approx -Le_d \tag{18}$$

3.4. System stability with disturbance observer

With the disturbance observer in (14), the control signal in (12) will become:

$$v = -h^{-1}(.)\left[\lambda e_p + T\dot{r}_D + \hat{d}\right] \tag{19}$$

or

$$\begin{aligned} v &= -h^{-1}(.)\lambda e_p - h^{-1}(.)\left[T\dot{r}_D + \hat{d}\right] \\ &= v_1 + v_2 \end{aligned} \tag{20}$$

where $v_1 = -h^{-1}(.)\lambda e_p; v_2 = -h^{-1}().\left[T\dot{r}_D + \hat{d}\right]$. Then the equation (6) will become:

$$\dot{e}_p = T\dot{r}_D + h(.)\left[-h^{-1}(.)\left[\lambda e_p + T\dot{r}_D + \hat{d}\right]\right] + d(.) \tag{21}$$

$$\dot{e}_p = -\lambda e_p + e_d \tag{22}$$

where $e_d = d - \hat{d}$ is disturbance estimation error The Lyapunov candidate function is chosen as:

$$V = \frac{1}{2}e_p^T e_p + \frac{1}{2}e_d^T e_d$$

Then the derivative of this function will be:

$$\begin{aligned} \dot{V} &= {e_p}^T \dot{e}_p + e_d^T \dot{e}_d = {e_p}^T\left(-\lambda e_p + e_d\right) + e_d^T\left(-Le_d\right) \\ &= \left(-e_p^T \lambda e_p + e_p^T e_d\right) + e_d^T\left(-Le_d\right) \\ &= -\left(\frac{1}{2}{e_p}^T e_p - e^T e_d + \frac{1}{2}e_d^T e_d\right) - \left(\lambda - \frac{1}{2}\right){e_p}^T e_p \\ &\quad - \left(L - \frac{1}{2}\right)e_d^T e_d \\ &= -\frac{1}{2}\left(e_p - e_d\right)^T\left(e_p - e_d\right) - \left(\lambda - \frac{1}{2}\right)e_p^T e_p - \left(L - \frac{1}{2}\right)e_d^T e_d \end{aligned}$$

If λ and L are chosen as $\lambda > 1/2$ and $L > 1/2$, then $\dot{V} < 0$. This means that the system is asymptotic stable according to Lyapunov theorem. e and e_d will converge to zero with the control law in (19) and the disturbance observer (14).

In (7), when $e_p = \begin{bmatrix} e_{p1} & e_{p2} \end{bmatrix}^T \to 0$, then

$$\lim_{e_p \to 0} h(.) = \begin{bmatrix} -\frac{r}{2} & -\frac{r}{2} \\ 0 & 0 \end{bmatrix}$$

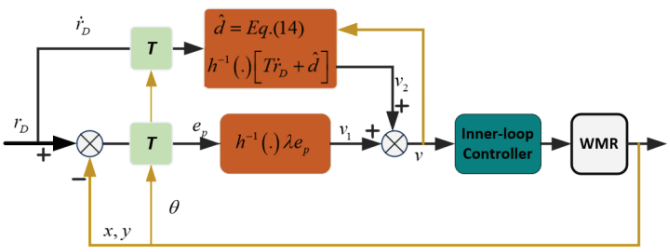

Figure 3. Diagram of outer-loop tracking controller

Hence $h(.)$ is not invertible, the calculation of the control signal v cannot be implemented. To resolve that problem, instead of using law as [33] in this research, the value of e_{p1} in (7) is introduced to be replaced by $e_{p1} = \delta \operatorname{sign}(e_{p1})$ as $e_{p1} \leq \delta$. This solution is consistent because the sign of e_{p1} directly affects the control signal v; the value of δ is select so that the wheel rotational speeds reach the minimum speed in case $e_{p1} \leq \delta$.

The detail diagram of the tracking controller with disturbance observer is depicted in Fig. 3.

4. Description of the Hardware and the Experimental Procedure

The block diagram for a WMR experimental control setup is shown in Fig. 4. In this setup, the outer loop controller is executed on the embedded computer. In which, the WMR position and orientation is determined by an ArUco marker and vision method. Based on these measurements, the adaptive controller with disturbance observer described in (19) is implemented to find the reference signals for the inner loop controller. The inner loop controller is executed on the microcontroller to control the rotational speed of the right and left driving wheel of robot.

The apparatus of WMR hardware, components and experimental control setup are shown in Fig. 5 to Fig. 7. In this setup, the IP camera is mounted on the top position so that it can cover the robot and its experimental trajectory. The robot position and orientation is detected by the ArUco marker that is placed at midpoint of driving wheels M.

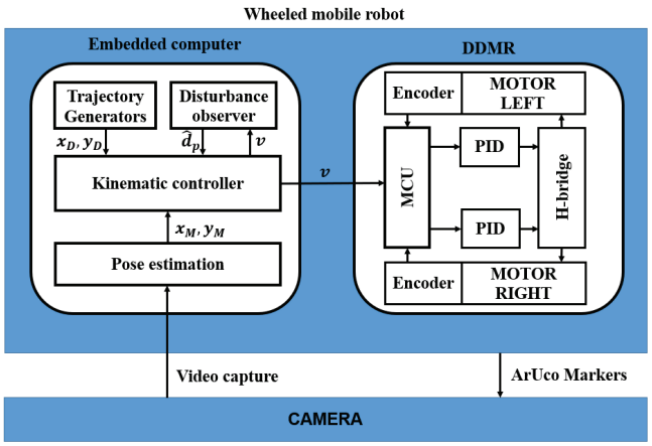

Figure 4. Block diagram of WMR experimental control implementation

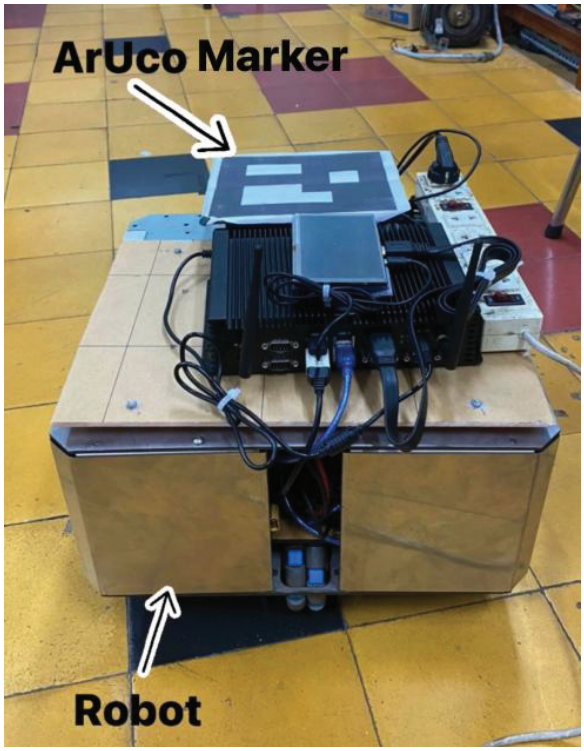

Figure 5. Apparatus of WMR with an ArUco marker and embedded computer

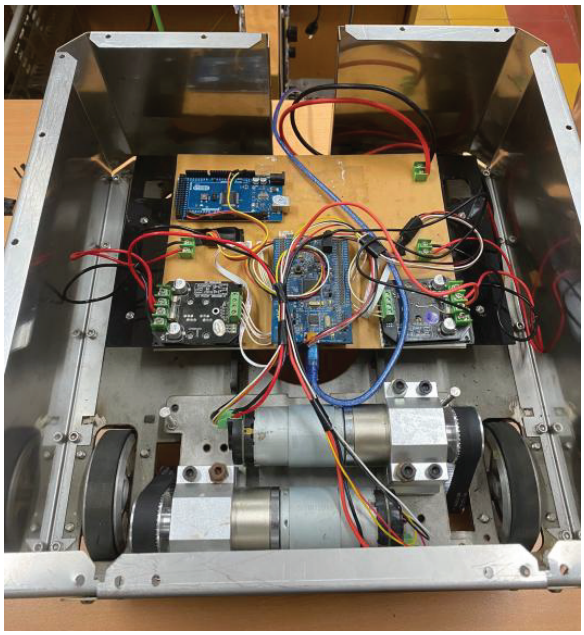

Figure 6. Setup of electric components in WMR

The experimental procedure involves the following steps:

(1) Deploy the PID controller for the robot's inner loop on the microcontroller.

(2) Set up the mounting frame for the IP camera and perform calibration using a checkerboard pattern.

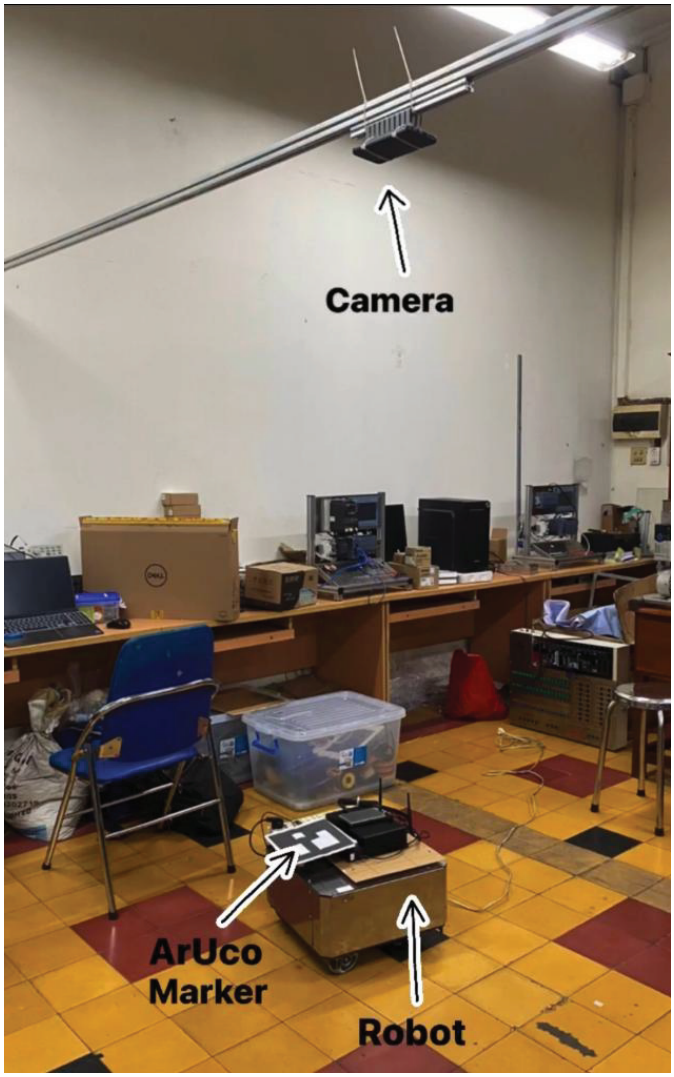

Figure 7. Overall image of experimental control setup

(3) Deploy the pose estimation program on the embedded computer to gather position data (x, y, θ) from the camera.

(4) Deploy the adaptive controller with a disturbance observer on the embedded computer.

(5) Position the robot at its initial point for trajectory tracking.

(6) Execute the programs through ROS.

(7) Collect the data and print the results.

(8) Stop the observation process by terminating the program.

5. Simulation and Experiment

To evaluate the proposed controller, it was tested in both simulation and experimental settings.

In the simulation, the WMR model and the proposed controller were implemented in MATLAB Simulink. Two trajectory cases were used to verify the simulation results: an eight-shaped trajectory and a circular trajectory. The mathematical expression for the eightshaped trajectory is presented in Equation (23), while the circular trajectory is described in Equation (24):

Table 1. Robot simulation parameters

Parameter	Description	Value
r	Wheel radius (m)	0.06
$2b$	Driving wheel distances (m)	0.31
m_G	Weight of robot flatform (kg)	10
m_W	Weight of robot wheel (kg)	0.7
	Distance of MG (m)	0.1
I_G	inertial moment of the platform about the vertical axis through point G (kg.m^2)	0.2
I_w	inertial moment of each wheel about its rotational axis (kg.m^2)	0.0013
I_D	inertial moment of each wheel about its diameter axis (kg.m^2)	0.0038

$$\begin{cases} x_d = \sin(0.1t) \\ y_d = \sin(0.2t) \end{cases} \quad (23)$$

$$\begin{cases} x_d = \cos(0.1t) \\ y_d = \sin(0.1t) \end{cases} \quad (24)$$

The simulation parameters for the WMR are set in the condition of our experiment robot as Table 1; and the controller parameters are set as $\lambda = \begin{bmatrix} 2 & 0 \\ 0 & 2 \end{bmatrix}$, $L = \begin{bmatrix} 100 & 0 \\ 0 & 100 \end{bmatrix}$. The load disturbances and uncertainty factors are set as: $\tau_d = \begin{bmatrix} 1+\sin(0.2t) \\ 1+\cos(0.2t) \end{bmatrix}$; $\dot{\gamma} = \begin{bmatrix} 0.2r\phi_R \sin(t) \\ 0.2r\phi_R \cos(t) \end{bmatrix}$; and $\dot{\eta} = 0.2\sin(t)$.

Simulation results are presented in Fig. 8 through Fig. 23, demonstrating the performance of the proposed controller on circular and eight-like trajectories. Additionally, the algorithm from [33] is evaluated for comparison with the proposed controller. The simulation results indicate that both controllers can effectively track the reference trajectories. Tracking

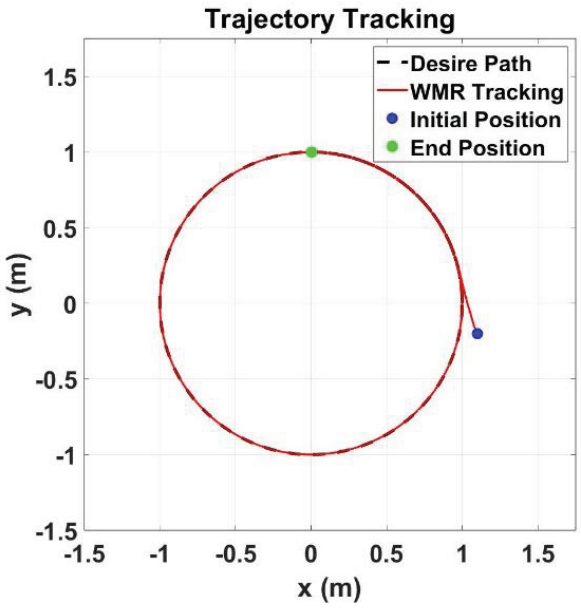

Figure 8. Circular trajectory tracking result by using proposed controller

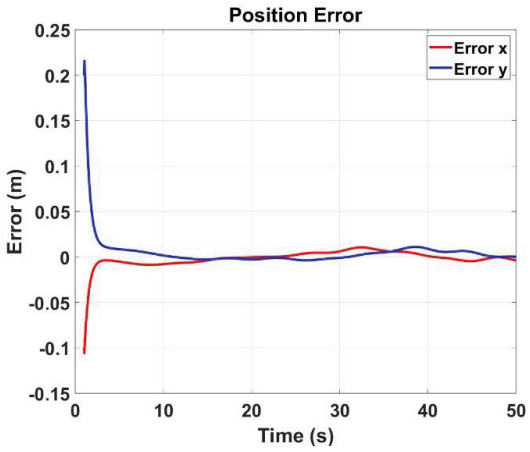

Figure 9. Circular trajectory tracking errors by using proposed controller

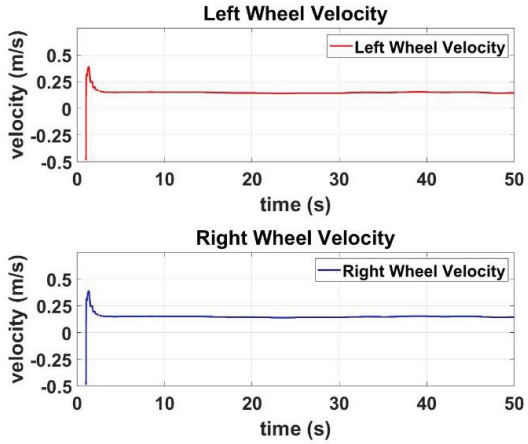

Figure 10. Reference speeds of driving wheels with respect to circular trajectory generated by proposed controller

errors for both controllers are shown in Fig. 9, Fig. 13, Fig. 17 and Fig. 21.

It is evident that the tracking errors in Fig. 9 and Fig. 17 converge smoothly to small values, while the controller from [33] exhibits significant sudden changes when the error is small, as shown in Fig. 13 and Fig. 21. This behavior is due to the discontinuous translation in the matrix $h(.)$ when $e_p \rightarrow 0$ in equation (19) changes.

The proposed controller's significant advantages over the one in [33] are evident in the wheel speed control signals (Fig. 10, Fig. 14, Fig. 18, and Fig. 22) and disturbance estimation results (Fig. 11, Fig. 15, Fig. 19 and Fig. 23).

It can be observed that the wheel velocities and estimated disturbances are stable and smooth with the proposed controller, whereas the controller in [33] exhibits large variations, particularly from the 47th second onward, as seen in Fig. 15, and Fig. 23. These variations may lead to system instability.

The simulation results confirm that the proposed controller performs effectively, exhibiting accurate-tracking, smooth responses, precise estimations, and overall system stability.

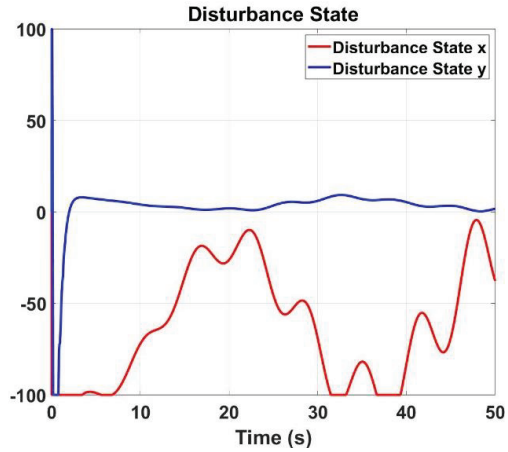

Figure 11. Disturbances estimation with respect to circular trajectory from proposed controller

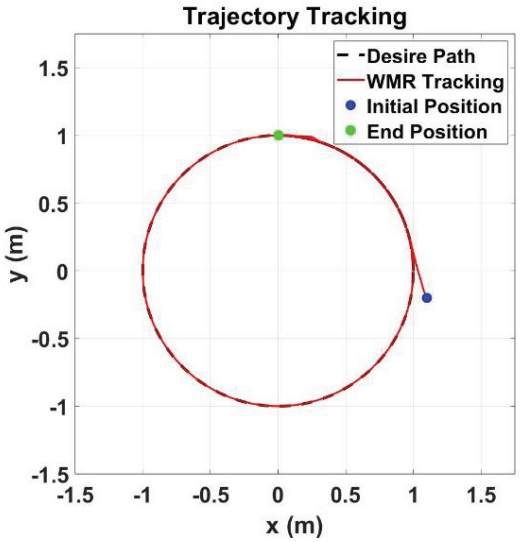

Figure 12. Circular trajectory tracking result by controller from [33]

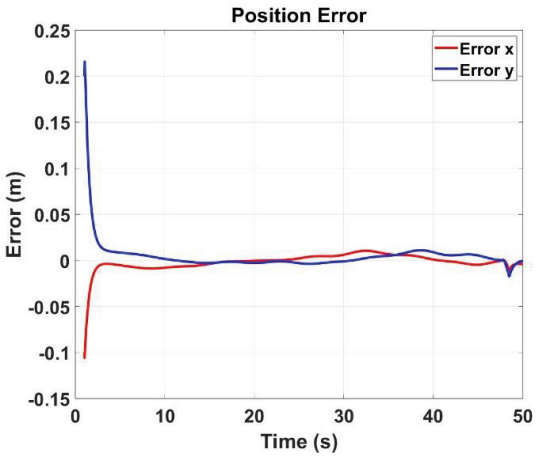

Figure 13. Circular trajectory tracking error by controller from reference [33]

Following the successful simulations, the proposed controller was implemented and tested under real-world conditions using a physical robot. In this

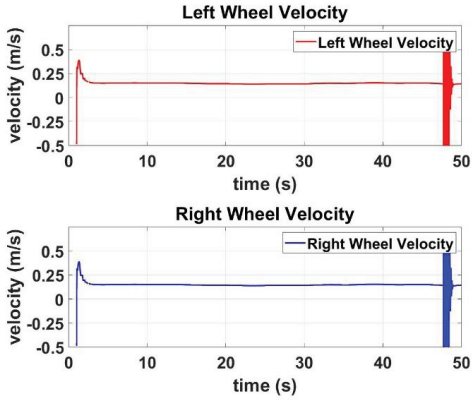

Figure 14. Reference speeds of driving wheels with respect to circular trajectory generated by controller from [33]

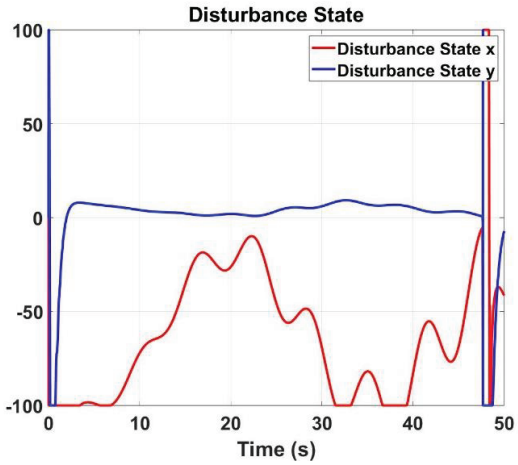

Figure 15. Disturbances estimation by controller from [33]

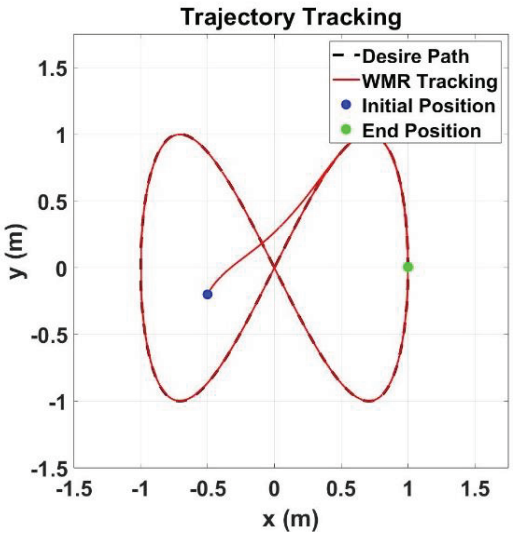

Figure 16. Eight-like trajectory tracking result by using proposed controller

experimental setup, the robot was tasked with tracking circular and square trajectories, both under no-load and 5 kg load conditions.

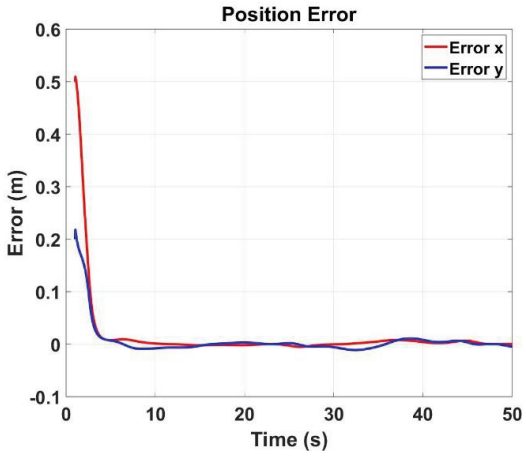

Figure 17. Eight-like trajectory tracking error with respect to eight-like by proposed controller

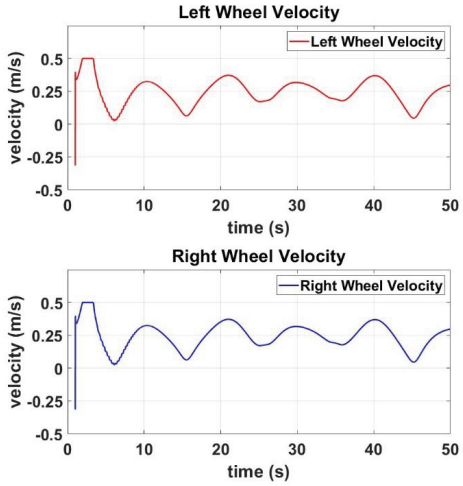

Figure 18. Reference speeds of driving wheels with respect to eight-like trajectory generated by proposed controller

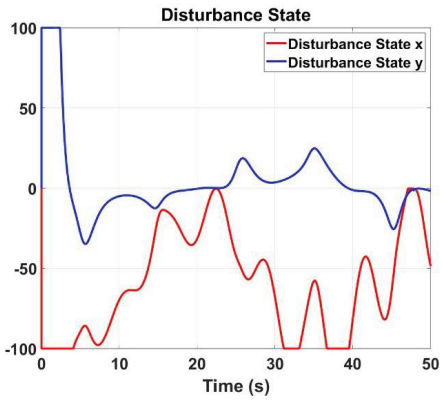

Figure 19. Disturbances estimation with respect to eight-like trajectory from proposed controller

Fig. 24 through Fig. 27 present the control results obtained from the real-world experiments. The results demonstrate that the controller successfully guides the robot along the circular trajectory (Fig. 24) with a small steady-state error of less than 3 cm (Fig. 25). The controller's output signals, represented by the

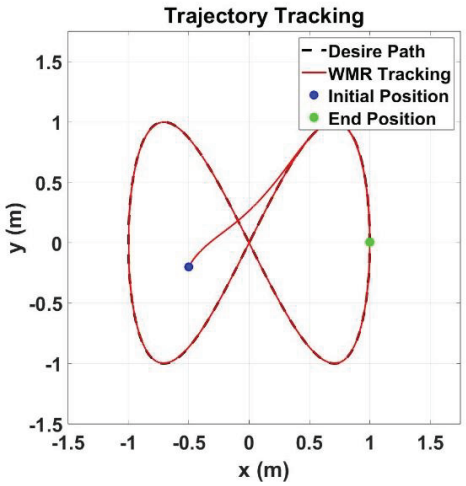

Figure 20. Eight-like trajectory tracking result by controller from [33]

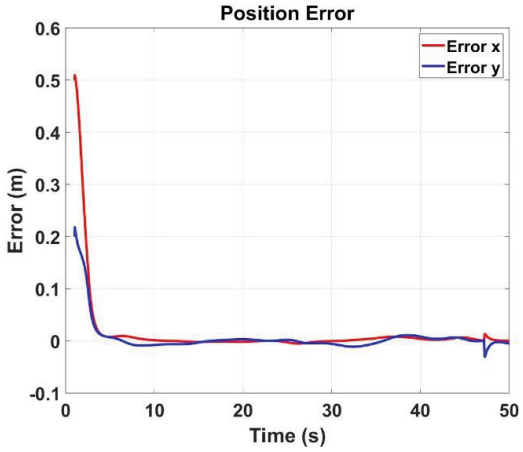

Figure 21. Eight-like trajectory tracking error by controller from reference [33]

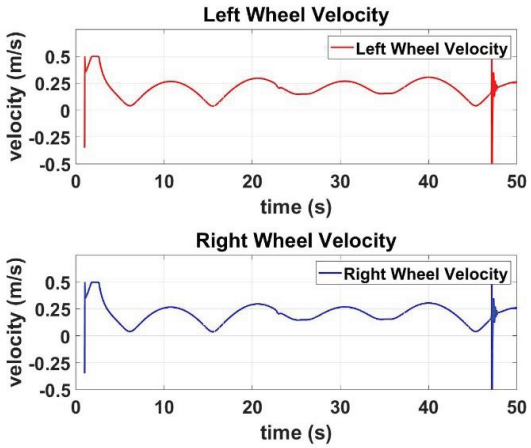

Figure 22. Reference speeds of driving wheels with respect to Eight-like trajectory generated by controller from [33]

wheel velocities, are shown in Fig. 26. For the circular trajectory, the right wheel appears to maintain a constant speed of 0.06 m/s, while the left wheel speed adjusts to follow the trajectory with smaller speed.

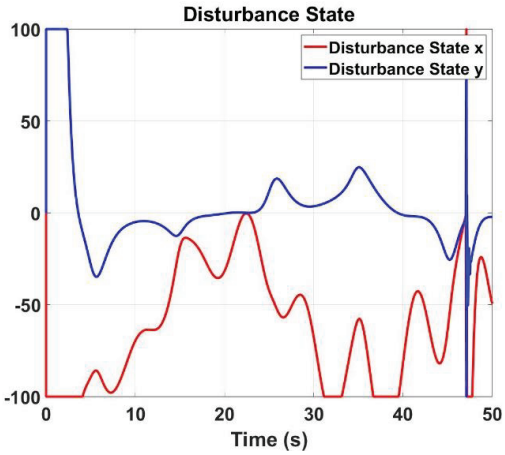

Figure 23. Disturbances estimation with respect to eight-like by controller from [33]

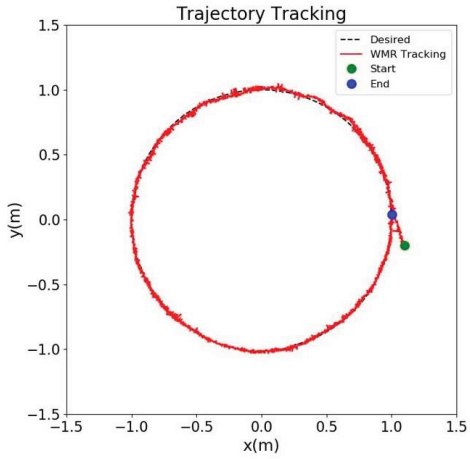

Figure 24. Experimental tracking result with respect to circular trajectory

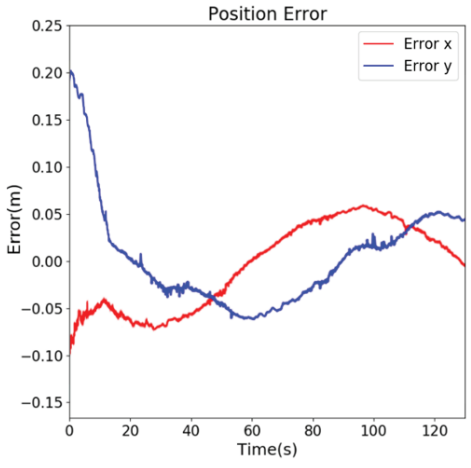

Figure 25. Experimental tracking errors with respect to circular trajectory

The disturbance estimation results are illustrated in Fig. 27.

Similarly, the control results for the square trajectory are shown in Fig. 28 through Fig. 31. Fig. 28 illustrates the tracking performance for the square trajectory. It can be observed that there is an overshoot

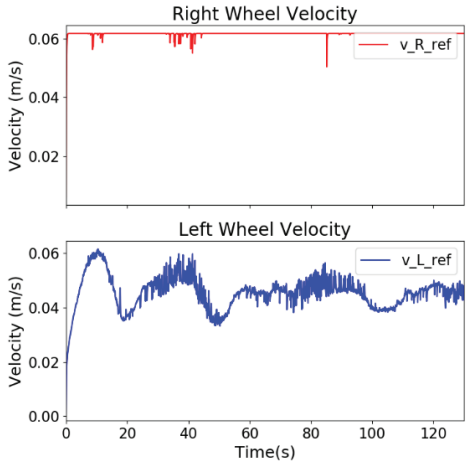

Figure 26. Experimental wheels velocity with respect to circular trajectory

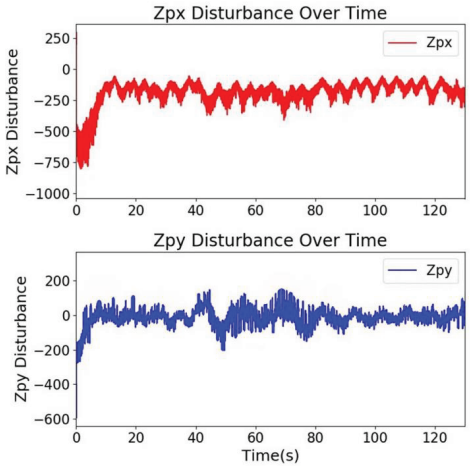

Figure 27. Experimental disturbances estimation with respect to circular trajectory

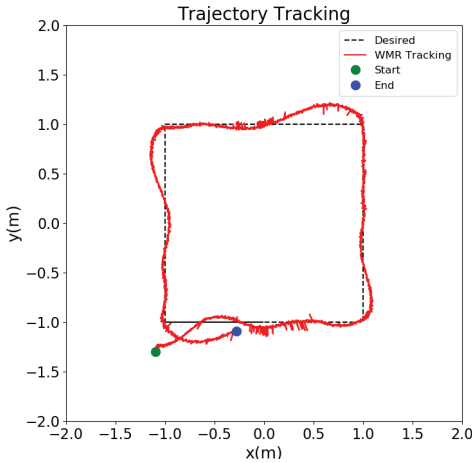

Figure 28. Experimental tracking result with respect to square trajectory

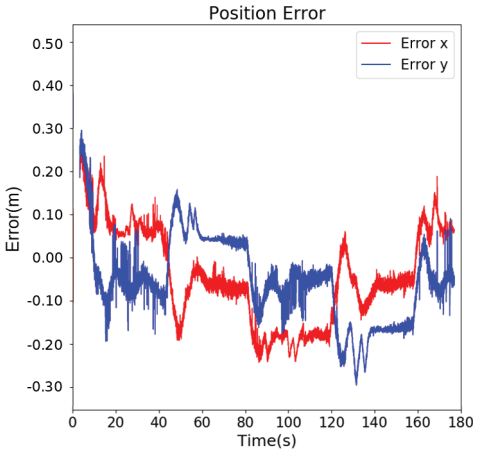

Figure 29. Experimental tracking error with respect to square trajectory

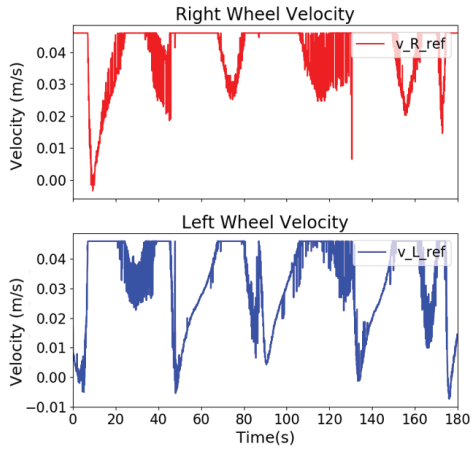

Figure 30. Experimental wheels velocity with respect to square trajectory

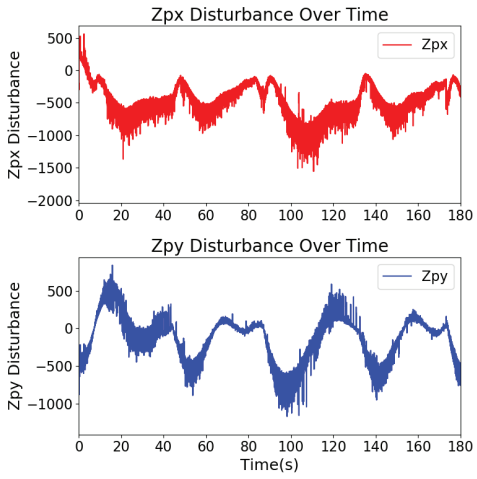

Figure 31. Experimental disturbances estimation with respect to square trajectory

when the reference changes its orientation, which occurs due to the robot's inertia and reference speed, causing it to continue moving forward until it adapts to the new orientation. Fig. 30 depicts the wheel speeds, showing that the left wheel speed decreases rapidly to accommodate the sudden change in the reference trajectory. The disturbance estimation results are presented in Fig. 31.

Finally, the controller is verified in long-time and load conditions. In this test, the robot carries a 5 kg

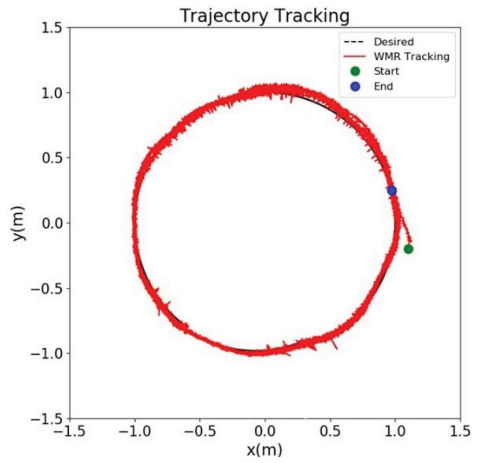

Figure 32. Experimental tracking result with respect to 4loops circular trajectory under 5 kg load

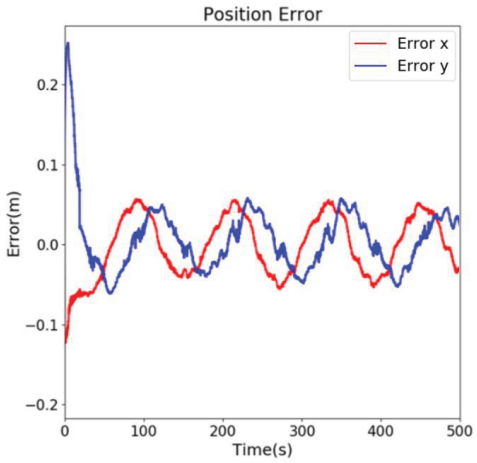

Figure 33. Experimental tracking errors with respect to 4loops circular trajectory under 5 kg load

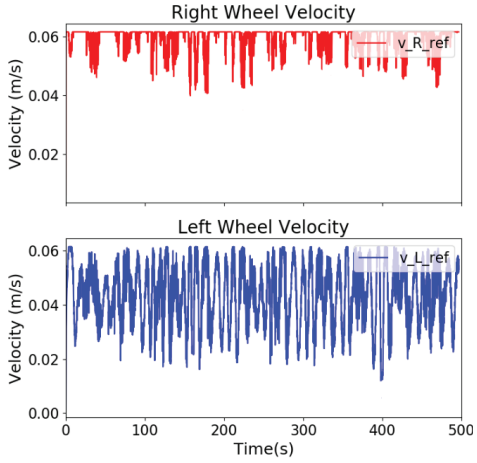

Figure 34. Experimental wheels velocity with respect to 4loops circular trajectory under 5 kg load

load and track to circular and square trajectories in 4-loops. The tracking results are shown in Fig. 32 and Fig. 35. It can be seen that the controller successfully adapts to varying load conditions. Furthermore, the control performances are kept stable in all loops, this demonstrates that the controller is stable and robust

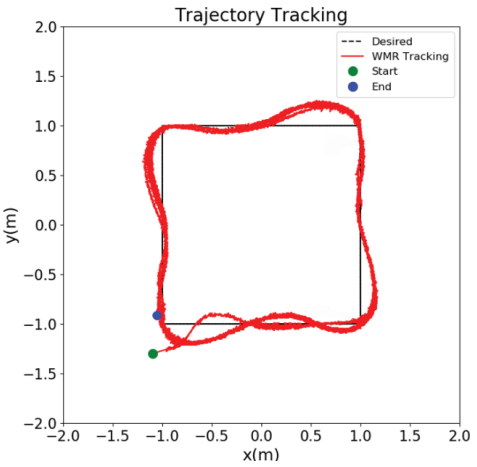

Figure 35. Experimental tracking result with respect to 4loops square trajectory under 5 kg load

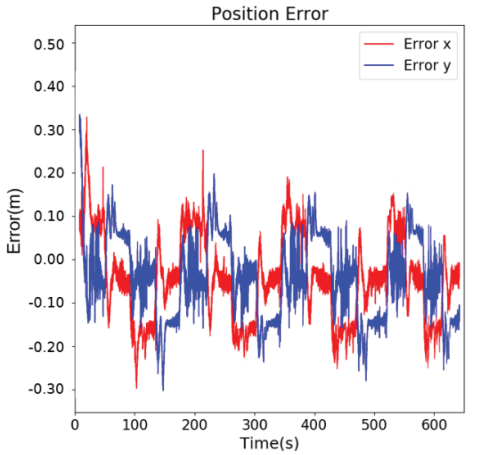

Figure 36. Experimental tracking errors with respect to 4loops square trajectory under 5 kg load

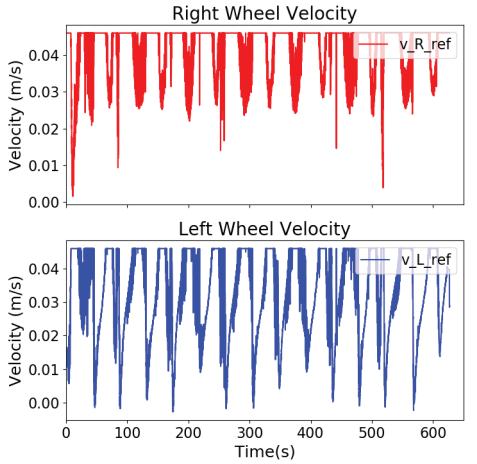

Figure 37. Experimental wheels velocity with respect to 4loops circular trajectory under 5 kg load

over time. The control signals with respect to trajectories, are displayed in Fig. 34 and Fig. 37. They show that the wheels' speeds are similar after each cycle. This proves the robustness and stability of the controller.

Finally, the proposed controller is tested under longduration and load conditions. In this experiment, the robot carried a 5 kg load while tracking circular and square trajectories over four loops. The tracking results are shown in Fig. 32 and Fig. 35. The results indicate that the controller adapts well under load conditions, maintaining stable control performance throughout all loops. This demonstrates the controller's stability and robustness over time. Furthermore, the control signals corresponding to the trajectories are displayed in Fig. 33 and Fig. 35, showing that the wheel speeds remain consistent after each cycle. This consistency further proves the robustness and stability of the controller.

6. Conclusion

In this research, a robust adaptive controller with a disturbance observer was investigated for nonholonomic robots, based on the kinematic and dynamic models of Wheeled Mobile Robots (WMRs). The disturbance observer was employed to handle system uncertainties and external disturbances. The stability of the proposed controller was proven using both Hurwitz and Lyapunov stability criteria.

The study primarily focuses on the outer loop tracking control scheme, which improves the performance of a previously proposed method by incorporating a disturbance handler and addressing remaining issues, such as providing a clear mathematical interpretation for non-invertible matrices and implementing this directly.

Moreover, extensive simulations and experimental results were conducted, demonstrating the proposed controller's efficiency, robustness, and stability.

ACKNOWLEDGEMENTS

This research is funded by Vietnam National University Ho Chi Minh City (VNU-HCM) under grant **number C2021-20-15** and by Ho Chi Minh City University of Technology - VNU-HCM under grant **number SVOISP-2023-ĐDT - 75**

We acknowledge the support of time and facilities from Ho Chi Minh City University of Technology (HCMUT), VNU-HCM for this study.

Authors' Contributions Trong Tai Nguyen conceived of the presented idea, developed the theory and performed the computations, prepared facilities for experimental, verified the analytical methods and results. Others conducted the experimental results, and data collection. All authors discussed the results and contributed to the final manuscript.

Declarations

Data Availability The authors confirm that the data supporting the findings of this study are available within the article and its Supplementary material. Raw data that support findings of this study are available from the corresponding author, upon the reasonable request.

Competing interests Not applicable

AUTHORS

Trong Tai Nguyen* – Faculty of Electrical & Electronics Engineering, Ho Chi Minh City University of Technology (HCMUT), 700000, Vietnam, e-mail: nttai@hcmut.edu.vn.

Doan Phuc An Nguyen – Faculty of Electrical & Electronics Engineering, Undergraduate School, Ho Chi Minh City University of Technology (HCMUT), Vietnam National University Ho Chi Minh City, 700000, Vietnam, e-mail: an.nguyen23112001@hcmut.edu.vn.

Dai Nghia Tran – Faculty of Electrical & Electronics Engineering, Undergraduate School, Ho Chi Minh City University of Technology (HCMUT),Vietnam National University Ho Chi Minh City, 700000, Vietnam, e-mail: nghia.tran.sherlock@hcmut.edu.vn.

Phuc Bao Nguyen Nguyen – Faculty of Electrical & Electronics Engineering, Undergraduate School, Ho Chi Minh City University of Technology (HCMUT), Vietnam National University Ho Chi Minh City, 700000, Vietnam, e-mail: nguyen.nguyenbao311003@hcmut.edu.vn.

Thanh Dat Mai – Faculty of Electrical & Electronics Engineering, Undergraduate School, Ho Chi Minh City University of Technology (HCMUT), Vietnam National University Ho Chi Minh City, 700000, Vietnam, e-mail: dat.maibk021@hcmut.edu.vn.

*Corresponding author

References

[1] R. Raj and A. Kos, "A Comprehensive Study of Mobile Robot: History, Developments, Applications, and Future Research Perspectives", Applied Sciences., vol. 12, no. 14, 2022. DOI: 10.3390/app12146951

[2] I. Doroftei and F. Adăscăliţei, "PRACTICAL APPLICATIONS FOR MOBILE ROBOTS BASED ON MECANUM WHEELS - A SYSTEMATIC SURVEY", The Romanian Review of Precision Mechanics, Optics and Mechatronics., no. 40, 2011, 21–29.

[3] C. Mireles, M. Sanchez, D. Cruz-Ortiz, I. Salgado, and I. Chairez, "Home-care nursing controlled mobile robot with vital signal monitoring", Medical & Biological Engineering & Computing., vol. 61, no. 2, 2023, 399–420. DOI: 10.1007/s11517-022-02712-y

[4] O. Buckmann, M. Krömker, and U. Berger, "An Application Platform for the Development and Experimental Validation of Mobile Robots for Health Care Purposes", Journal of Intelligent and Robotic Systems., vol. 22, no. 3, 1998, 331–350. DOI: https://doi.org/10.1023/A:1007945702881

[5] R. Galati, G. Mantriota, and G. Reina, "Adaptive heading correction for an industrial heavy-duty omnidirectional robot", (in eng), Sci Rep., vol. 12,

no. 1, 2022, 19608. DOI: 10.1038/s41598-022-24270-x

[6] C. Patruno, V. Renò, M. Nitti, N. Mosca, M. di Summa, and E. Stella, "Vision-based omnidirectional indoor robots for autonomous navigation and localization in manufacturing industry", Heliyon., vol. 10, no. 4, p. e26042, 2024. DOI: 10.1117/12.2595511

[7] J. P. Trevelyan, S.-C. Kang, and W. R. Hamel, "Robotics in Hazardous Applications", in Springer Handbook of Robotics., B. Siciliano and O. Khatib, Heidelberg: Springer Berlin Heidelberg, 2008, 1101–1126. DOI: 10.1007/978-3-319-32552-1_58

[8] H. Taheri and C. X. Zhao, "Omnidirectional mobile robots, mechanisms and navigation approaches," Mechanism and Machine Theory., vol. 153, 2020, 103958. DOI: 10.1016/j.mechmachtheory.2020.103958

[9] L. Wijayathunga, A. Rassau, and D. Chai, "Challenges and Solutions for Autonomous Ground Robot Scene Understanding and Navigation in Unstructured Outdoor Environments: A Review", *Applied Sciences*., vol. 13, no. 17. DOI:10.3390/app13179877

[10] S. A. Ahmed and M. G. Petrov, "Trajectory Control of Mobile Robots using Type-2 Fuzzy-Neural PID Controller", IFAC-PapersOnLine., vol. 48, no. 24, 2015. DOI: https://doi.org/10.1177/09596518251322228

[11] K. Al-Mutib and F. Abdessemed, "Indoor mobile robot navigation in unknown environment using fuzzy logic based behaviors", Adv. Sci. Technol. Eng. Syst. J., vol. 2, no. 3, 327–337, 2017. DOI: https://dx.doi.org/10.25046/aj020342

[12] Y.-H. Chen and Y.-Y. Chen, "Nonlinear Adaptive Fuzzy Control Design for Wheeled Mobile Robots with Using the Skew Symmetrical Property", Symmetry., vol. 15, no. 1. DOI: 10.3390/sym15010221

[13] G. Zidani, S. Drid, L. Chrifi-Alaoui, A. Benmakhlouf, and S. Chaouch, "Backstepping controller for a wheeled mobile robot", in 2015 4th International Conference on Systems and Control (ICSC), 2015, 443–448. DOI: 10.1109/ICoSC.2015.7153286

[14] G. Yanfeng, Z. Hua, and Y. Yanhui, "Back-Stepping and Neural Network Control of a Mobile Robot for Curved Weld Seam Tracking", Procedia Engineering., vol. 15, 2011, 38–44. DOI: https://doi.org/10.1016/j.proeng.2011.08.009

[15] M. A. Moqbel Obaid, A. R. Husain, and A. A. Mohammed Al-kubati, "Robust Backstepping Tracking Control of Mobile Robot Based on Nonlinear Disturbance Observer", International Journal of Electrical and Computer Engineering (IJECE)., vol. 6, no. 2, 2016. DOI: 10.11591/ijece.v6i2. pp. 901–908

[16] S. A. Tchenderli-Baham, F. Hamerlain, and N. Saadia, "Adaptive sliding mode for the control of a wheeled mobile robot", in 2015 15th International Conference on Control, Automation and Systems (ICCAS), 2015, 699–703. DOI: https://doi.org/10.1109/ICCAS.2015.73650

[17] Y. Jinhua, Y. Suzhen, and J. Xiao, "Trajectory Tracking Control of WMR Based on Sliding Mode Disturbance Observer with Unknown Skidding and Slipping", in 2017 2nd International Conference on Cybernetics, Robotics and Control (CRC), 2017, 18–22. DOI: 10.1109/CRC.2017.40

[18] A. Filipescu, V. Minzu, B. Dumitrascu, and E. Minca, "Trajectory-tracking and discrete-time sliding-mode control of wheeled mobile robots", in 2011 IEEE International Conference on Information and Automation, 2011, 27–32. DOI: 10.1109/ICINFA.2011.5948958

[19] J. Meng, H. Xiao, L. Jiang, Z. Hu, L. Jiang, and N. Jiang, "Adaptive Model Predictive Control for Mobile Robots with Localization Fluctuation Estimation", (in eng), Sensors (Basel)., vol. 23, no. 5, 2023. DOI: https://doi.org/10.3390/s23052501

[20] L. Jiang, S. Wang, Y. Xie, S. Q. Xie, S. Zheng, and J. Meng, "Fractional robust finite time control of four-wheel-steering mobile robots subject to serious time-varying perturbations", Mechanism and Machine Theory., vol. 169, 2022,104634. DOI: 10.1016/j.mechmachtheory.2021.104634

[21] İ. Ünal, Ö. Kabaş, O. Eceoğlu, and G. Moiceanu, "Adaptive Multi-Robot Communication System and Collision Avoidance Algorithm for Precision Agriculture", Applied Sciences., vol. 13, no. 15, 2023, 8602. DOI: https://doi.org/10.3390/app13158602

[22] Z. Cao, J. Song and Y. Niu, "Finite-time sliding mode control of Markovian jump systems subject to actuator nonlinearities and its application to wheeled mobile manipulator", Journal of the Franklin Institute., vol. 355, no. 16, 2018, 7865-7894. DOI: 10.1109/TAC.2019.2926156

[23] L. Ding, S. Li, Y. J. Liu, H. Gao, C. Chen, and Z. Deng, "Adaptive Neural Network-Based Tracking Control for Full-State Constrained Wheeled Mobile Robotic System", IEEE Transactions on Systems, Man, and Cybernetics: Systems., vol. 47, no. 8, 2017, 2410–2419. DOI: 10.1109/TSMC.2017.2677472

[24] K. Shojaei, "Neural adaptive output feedback formation control of type (m, s) wheeled mobile robots," IET Control Theory & Applications., vol. 11, no. 4, 2017, 504–515. DOI: https://doi.org/10.1049/iet-cta.2016.0952

[25] Z. Peng, S. Yang, G. Wen, A. Rahmani, and Y. Yu, "Adaptive distributed formation control for multiple nonholonomic wheeled mobile robots", Neurocomputing.,

vol. 173, 2016, 1485–1494. DOI: https://doi.org/10.1016/j.neucom.2015.09.022

[26] M. Begnini, D. W. Bertol, and N. A. Martins, "A robust adaptive fuzzy variable structure tracking control for the wheeled mobile robot: Simulation and experimental results", Control Engineering Practice, vol. 64, 2017, 27–43. DOI: https://doi.org/10.1016/j.conengprac.2017.04.006

[27] L. Xin, Q. Wang, J. She, and Y. Li, "Robust adaptive tracking control of wheeled mobile robot", Robotics and Autonomous Systems., vol. 78, 2016, 36–48. DOI: https://doi.org/10.1016/j.robot.2016.01.002

[28] H. Fang, Y. Zhu, S. Dian, G. Xiang, R. Guo, and S. Li, "Robust tracking control for magnetic wheeled mobile robots using adaptive dynamic programming", ISA Transactions., vol. 128, 2022, 123–132. DOI: 10.1016/j.isatra.2021.10.017

[29] S. Peng and W. Shi, "Adaptive Fuzzy Output Feedback Control of a Nonholonomic Wheeled Mobile Robot", IEEE Access., vol. 6, 2018,. DOI:10.1109/ACCESS.2018.2862163

[30] J. T. Huang and Y. L. Sung, "Adaptive beck-stepping dynamic surface tracking control of nonholonomic mobile robots", in 2016 IEEE 11th Conference on Industrial Electronics and Applications (ICIEA), 2016, 1026–1031. DOI: 10.1109/ICIEA.2016.7603733

[31] D. E. Kim, H. N. Yoon, K. S. Kim, M. S. Sreejith, and J. M. Lee, "Using current sensing method and fuzzy PID controller for slip phenomena estimation and compensation of mobile robot," in 2017 14th International Conference on Ubiquitous Robots and Ambient Intelligence (URAI), 2017, 397–401. DOI: 10.5772/intechopen. 110497

[32] M. Chen, "Disturbance Attenuation Tracking Control for Wheeled Mobile Robots With Skidding and Slipping", IEEE Transactions on Industrial Electronics., vol. 64, no. 4, 2017, pp. 3359–3368. DOI: 10.1109/TIE.2016.2613839

[33] N. T.-T. Vu, L. X. Ong, N. H. Trinh, and S. T. Huong Pham, "Robust adaptive controller for wheel mobile robot with disturbances and wheel slips", International Journal of Electrical and Computer Engineering (IJECE)., vol. 11, no. 1, 2021, 11. DOI: 10.11591/ijece.v11i1. pp336–346

[34] W. H. Chen, J. Yang, L. Guo, and S. Li, "Disturbance-Observer-Based Control and Related Methods–An Overview", IEEE Transactions on Industrial Electronics., vol. 63, no. 2, 2016, 1083–1095. DOI: 10.1109/TIE.2015.2478397